Final Technical Report

Project Title: "High Efficiency Solar Power via Separated Photo and Voltaic Pathways"

Covering Period: January 1, 2008 – November 30, 2008

Date of Report: February 13, 2009

Recipient: Solasta Inc.

Award Number: DE-FG36-08GO18013.A000

Working Partners: none

Cost-Sharing Partners: none

Contacts:

Claudia Moreno
Phone: 617-307-5031
Fax: 617-558-8616
Email: claudia.moreno@solastacorp.com

Michael J. Naughton (PI)
Phone: 617-307-5031
Fax: 617-558-8616
mike.naughton@solastacorp.com

DOE Project Team:

DOE Field Contracting Officer	-	Andrea Lucero
DOE Field Project Officer	-	Brad Ring
Project Engineer	-	Leon Fabick

Executive Summary:

The objective of this project is to demonstrate a novel nanostructured solar cell concept capable of achieving high efficiency levels that is relatively simple and inexpensive to manufacture. The high efficiency will be achieved by the novel structure that separates the path of the photons from the path of the generated charge carriers.

Our technology provides a photovoltaic medium with independent optical and electronic pathways, separating the *photo* from the *voltaic* with respect to required thickness of photovoltaic absorber material. It does so with innovations in both light and charge collection. For the former, the well-known electromagnetic transmission properties of coaxial wires (broadband transmission, low loss, TEM-mode propagation) are exploited for the first time in the visible regime, using the Solasta optical *nanocoax* as described below. For the latter, the PV layer separating the inner and outer conductors of the nanocoax is made thinner than all charge carrier diffusion lengths (electron, hole, exciton), significantly reducing recombination and phonon energy losses.

Significant Accomplishments:

Task	Task Objectives	Task Accomplishments	% Complete
1-1: Characterize Photovoltaic Performance of Solasta Solar Cell	Establish baseline efficiency performance and identify loss sources	We had previously characterized the baseline efficiency performance of solar cells fabricated in our proprietary architecture. We have eliminated some of the sources of loss identified in the previous quarter, and have made improvements in others. *As of 11/30/08, we will have evaluated various external quantum efficiency measurement apparati, determined the best option, and placed an order for such. Decision: Model QE-PV-SI from Newport Corp. We will also have initiated evaluation of various transparent conductive coating options for optimized conformality, conductivity, and transparency, and begun investigative collaborations with university and industry partners.*	*35%*
1-2: Model and Simulate Nanocoax Array Architecture and Performance	Use predictive power of computer simulation to guide selection of materials and nanocoax architecture	We had previously modified the FDTD codes for electromagnetic properties of solar cells in our architecture. *As of 11/30/08, we will have tested the aforementioned modified code in a single prototypical nanocoax structure, for monochromatic light.*	*20%*
1-3: Vary Photovoltaic Silicon Properties	Selection of proper preparation conditions for maximum silicon PV performance within the Solasta architecture	We had previously explored the parameter space for our PECVD system which leads to improved conformality of our amorphous silicon deposited on our carbon nanofibers.	*15%*
1-4: Introduce Dopant Materials into Silicon PV	Selection of proper junction configuration (*n-p*, *n-i-p*, etc.) for maximum silicon PV performance within the Solasta architecture	We had previously completed the introduction of chemical dopants to the amorphous silicon deposition system, and are now able to run processes with *p* and *n* doping gases. We have not yet performed enough systemic studies to determine optimal deposition conditions. *As of 11/30/08, we will have fabricated an initial nanocoax sample set incorporating a modified doping level in the n-window layer, in an attempt to increase its transparency.*	*10%*

Additional Detail:

To characterize and improve the baseline performance of the our cells, identify sources of efficiency loss in them, select the proper preparation conditions for maximum silicon PV performance, introduce dopant materials into this silicon PV medium, and investigation selection of the proper junction configuration for maximum silicon PV performance within the Solasta architecture, we have prepared several iterations of nanocoax solar cells, varying the properties of each constituent step. Some of these steps correspond to activities under Tasks 1-1 through 1-4, while others relate to multiple Tasks. The steps are simplified below. As it is not possible to show all results obtained during the project period in this report, we provide instead representative data that demonstrate the progression of overall effort and the results achieved.

1. Substrate; 2. Arrays; 3. Bottom Contact; 4. PV; 5. Top Contact; 6. Cells; 7. Simulation

1. Substrate

Glass, silicon, aluminum, and stainless steel substrates were investigated, with alumino-silicate high temperature glass (e.g. Corning 1737) and silicon chosen for further use.

2. Arrays

Many of the aforementioned iterations involved improving the quality of the carbon nanotube arrays, with regard to height, diameter, spacing, rigidity, straightness, purity, regularity (in height and diameter), and defect density (extrinsic and intrinsic; nanoscopic, microscopic, and macroscopic).

The preparation of vertically-aligned CNT arrays begins with an array of catalyst particles from which CNTs will be subsequently grown via PECVD. As the PECVD growth requires a conducting substrate, the first step is to deposit a conductive coating on the substrate. This can be any conductor that survives the thermal environment of the CVD chamber (600-700C), but there is an added constraint for the classic coax arrays: the conductor must be largely transparent after CNT growth. A substantial amount of effort was expended characterizing different conductive coatings of varying thickness, in order to strike a balance between sufficient conductivity for CNT growth and sufficient transparency. Obvious candidates such as conventional transparent conductive oxides, such as indium tin oxide (ITO), indium zinc oxide (IZO) and zinc oxide (ZnO) were investigated, but none proved capable of surviving the PECVD process. Colleagues at NREL (D. Ginley) have suggested that Nb-doped IZO could be a candidate, but we have yet to complete an investigation of this material. Instead, we have employed thin films of Ti and Cr as candidate conductors. Investigations of the transparency and conductivity of both materials as functions of film thickness were undertaken, with the following conclusions:

a. Ti was chosen as overall more appropriate than Cr, and
b. a maximum of 10 nm thickness Ti film maintains both reasonable conductivity and transparency.

In fact, we found that, if thinner Ti films could be employed with respect to the conductivity, such as 3-5 nm, we could achieve nearly 100% transparency after CNT growth by oxidizing the film into TiO, a transparent dielectric. Thus, effort was expended to find the thinnest possible film that would still facilitate PECVD CNT growth.

After Ti deposition, the CNT catalyst is deposited. Candidate catalysts include Fe, Ni, and Co. From previous experience with CNTs, we chose Ni. Ni nanodots arrays of the appropriate size and spacing for our use can be prepared by a number of techniques, including electron beam nanolithography, microsphere nanolithography, interference lithography, etc. Microsphere lithography involves an array of micron-scale polystyrene (or other appropriate material) spheres, self-assembled on the surface of a liquid, transferred to a substrate and dried. See Figure 1(a). Catalyst material (Ni) is then deposited through the voids between the spheres, leaving a kagome (honeycomb) pattern of nanodots after the spheres are washed away, Figure 1(b). While a somewhat tedious process requiring great diligence, this technique is capable of templating large area arrays (up to 100 cm^2 of more).

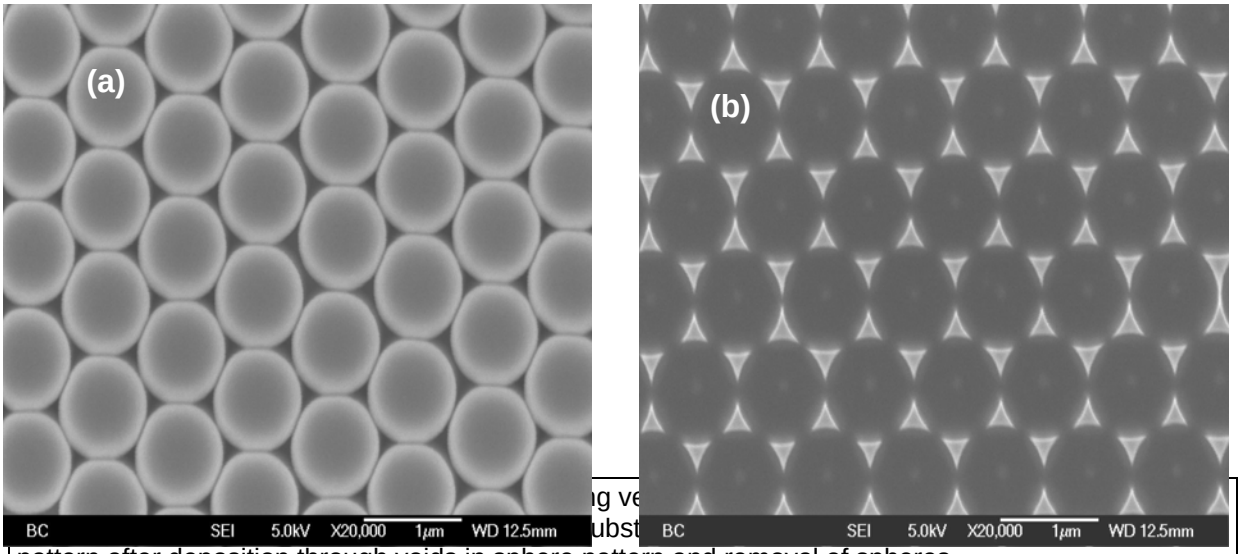

ubst
pattern after deposition through voids in sphere pattern and removal of spheres.

It is, however, nontrivial to prepare these arrays completely defect-free. We have characterized our array quality with optical and electron microscopy, and developed protocols that minimize the number and type of defect. Figure 2 below shows representative bright (left) and dark (right)-field optical microscope images of 1.5 μm-diameter polystyrene sphere arrays (upper set) and Ni-dot arrays deposited through a different such sphere array. Notice that the lower set is less defected than the upper. The rather macroscopic defects in the former can lead to severe leakage, and attempts were made at every stage to minimize their number.

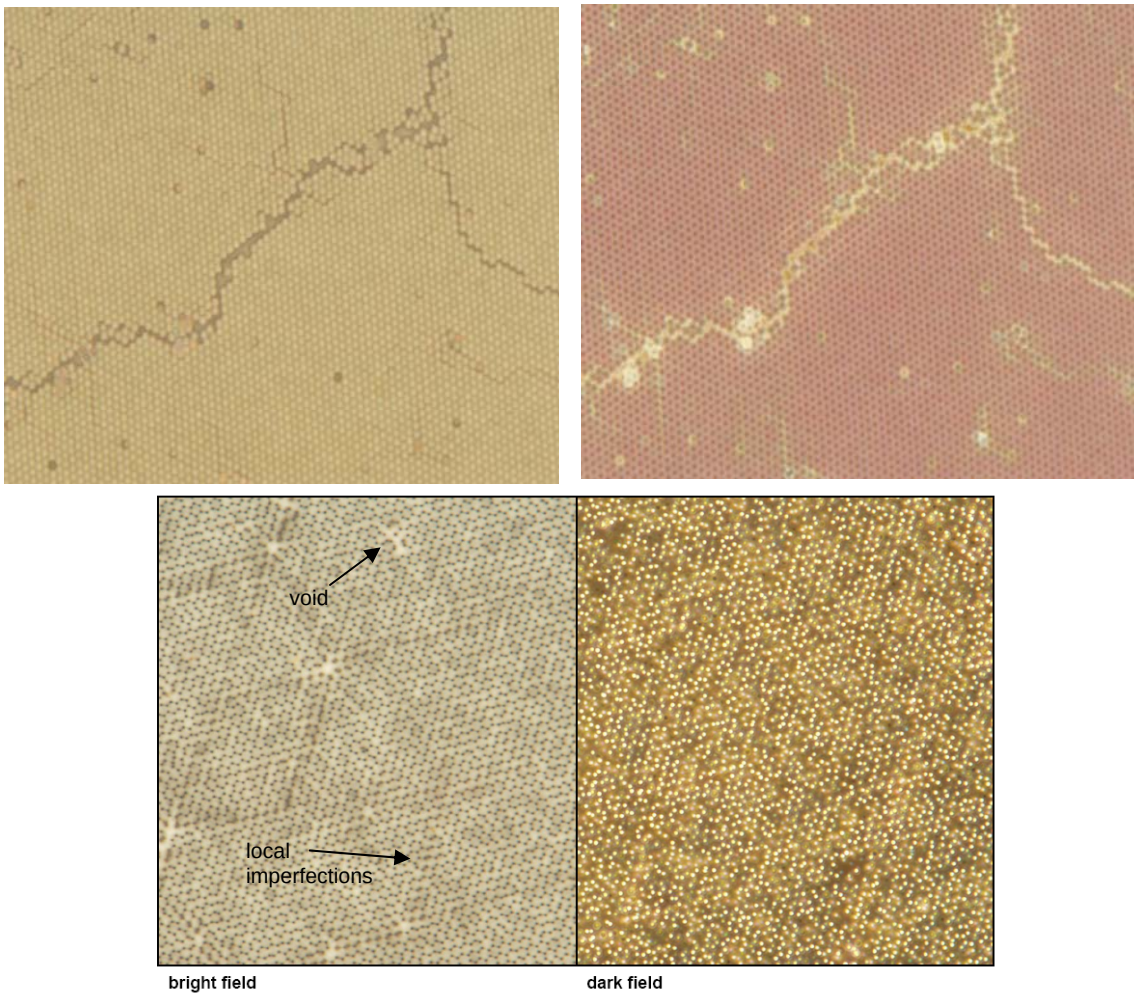

Fig. 2 Bright and dark-field optical microscope images of (upper) polystyrene microsphere arrays, and (lower) subsequent Ni-nanodot arrays, showing various types of defects and lattice imperfections possible with microsphere nanolithography.

The Ni on Ti pattern in Fig. 1(b) as prepared, however, is insufficient for high quality CNT array growth. This is because there can be too little or too much Ni to yield a single multi-walled CNT at each growth site. As examples, Figure 3 show what can happen when growth is attempted on a Ni substrate. One problem is the appearance of multiple CNTs that grow at each lattice site, each one being too short and/or too thin for our purposes (top left image). Another problem is the presence of small nanotubes/nanofibers not only at each catalyst site, but in between CNT sites (remaining images). These “satellite” CNTs proved to be deleterious to solar cell performance, by being inhomogeneously coated by subsequent bottom contact, PV and top contact films, ultimately leading to electrical shorts. An example of an etched and annealed lattice is shown in Fig. 4.

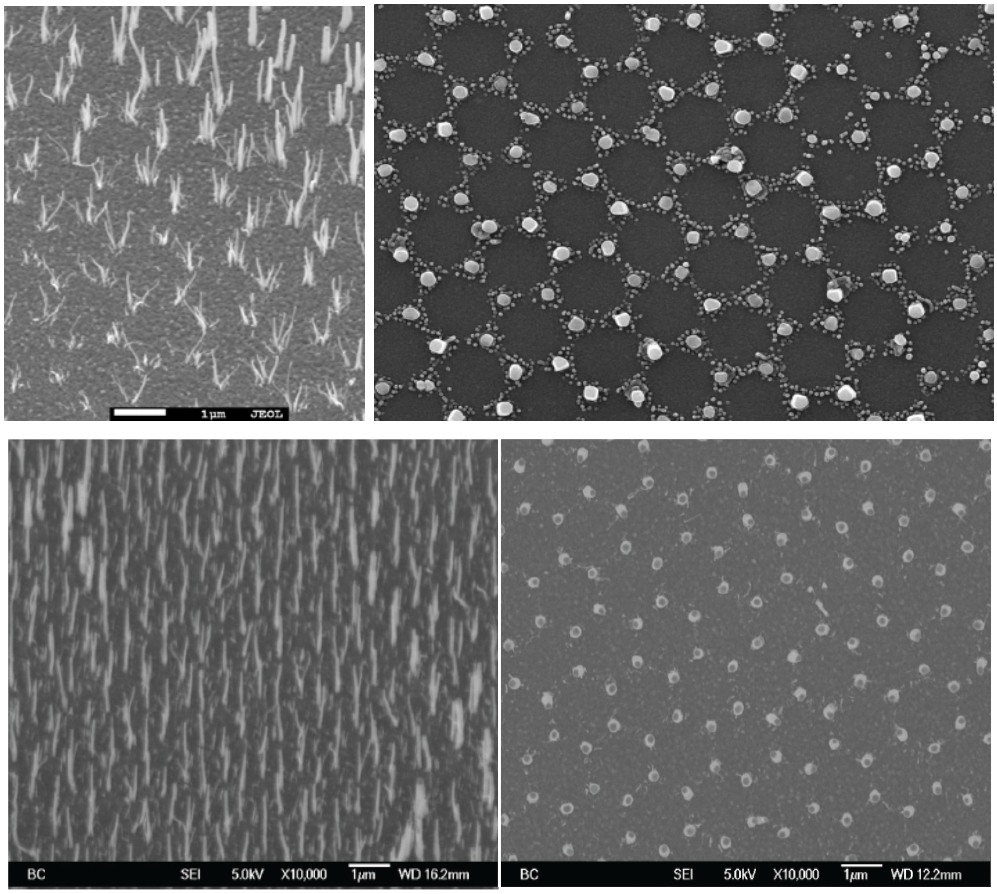

Fig. 3 PECVD growth of CNTs off as-deposited Ni catalyst sites, resulting in multiple CNTs per site (top left SEM image), or satellite CNTs between lattice sites (other SEM images).

Extensive effort was expended to clean up these arrays by reducing or eliminating the satellites and thereby improve the baseline performance of the solar cell. The array in Fig. 5 below is representative of the result of this effort, though it can be seen there that a small number of satellites still remains even there. In order to minimize or eliminate these satellites, or at least render them inactive, such that their presence, at least in small amounts, does not so deleteriously affect the performance of the nanocoax solar cell, additional new processes were developed. The most successful of these was the introduction of a dielectric layer applied after the CNT growth step. This served to coat the satellites and smooth out their rough edges, such that subsequent coatings of metals and PV were no longer presented sharp surfaces, so that top and bottom contact layers no longer shorted. The most successful dielectric layer was spin-on-glass (SOG). We extensively tested various forms of methyl-siloxane SOG, such as Honeywell Accuglass 312B and 512B, including testing a number of spin speeds and times, under various dilutions to vary the viscosity, and established a working protocol going forward.

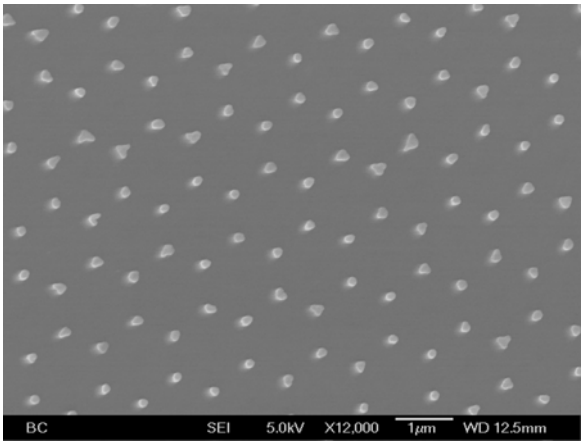

Fig. 4 Ni dot lattice after annealing and etching in ammonia gas, resulting in controlled dot size (area and volume), thus improving CNT arrays but restricting growth to a single CNT per lattice site.

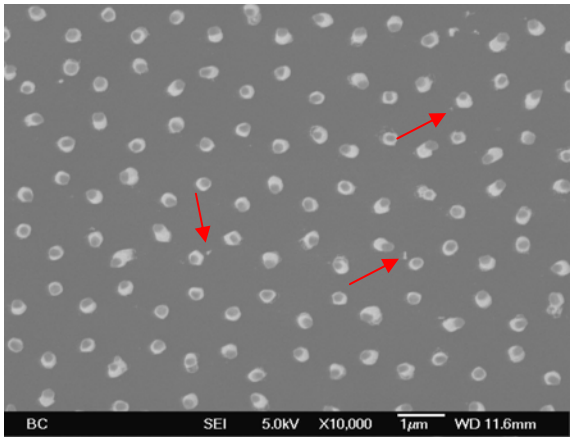

Fig. 5 SEM of PECVD-grown CNT array after controlling the size of the Ni catalyst nanodots. Some satellite CNTs, which have been found to diminish cell performance via electrical shorts remain, remain, as indicated.

3. Bottom Contact

Figure 6 below shows the result of a SOG film over the CNT array: the satellites are either smoothed over or buried. Once this SOG coating is employed, however, any remnant of a conducting substrate is lost, and so the entire array needs to be coated with an appropriate metal (it turns out the top 80% or so the CNTs do not get coated by the SOG, and remain bare). Moreover, the use of SOG may preclude the use of the classic coax configuration, depending on its final transparency, thus restricting further development to the distributed configuration. This new metal coating will play the role of the bottom contact of the distributed nanocoax solar cell. We investigated a number of such metals, including ITO, Al, Ag, Au, Cr, and Ti, deposited by various techniques such as sputtering, thermal evaporation and electron beam evaporation, and of various thicknesses between 5 and 100 nm. We ultimately chose 50 nm Ag via e-beam evaporation, based on studies of numerous completed solar cells.

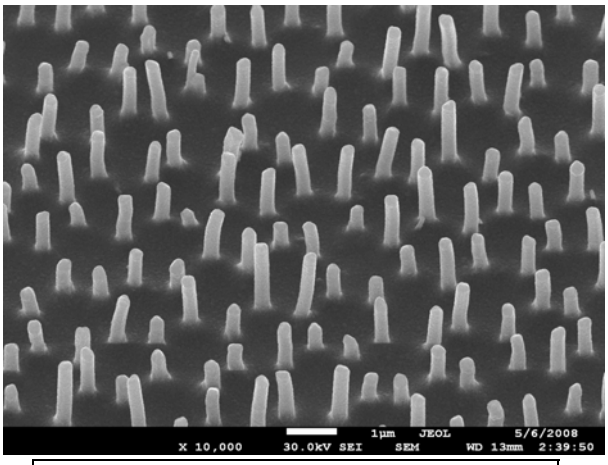

Fig. 6 CNT array after coating with SOG.

4. PV

The next step in the fabrication of a nanocoax solar cell is the deposition of the PV medium. We have chosen amorphous silicon, *a*-Si, and built a PECVD system in for this purpose. This chamber is shown in Figure 7.

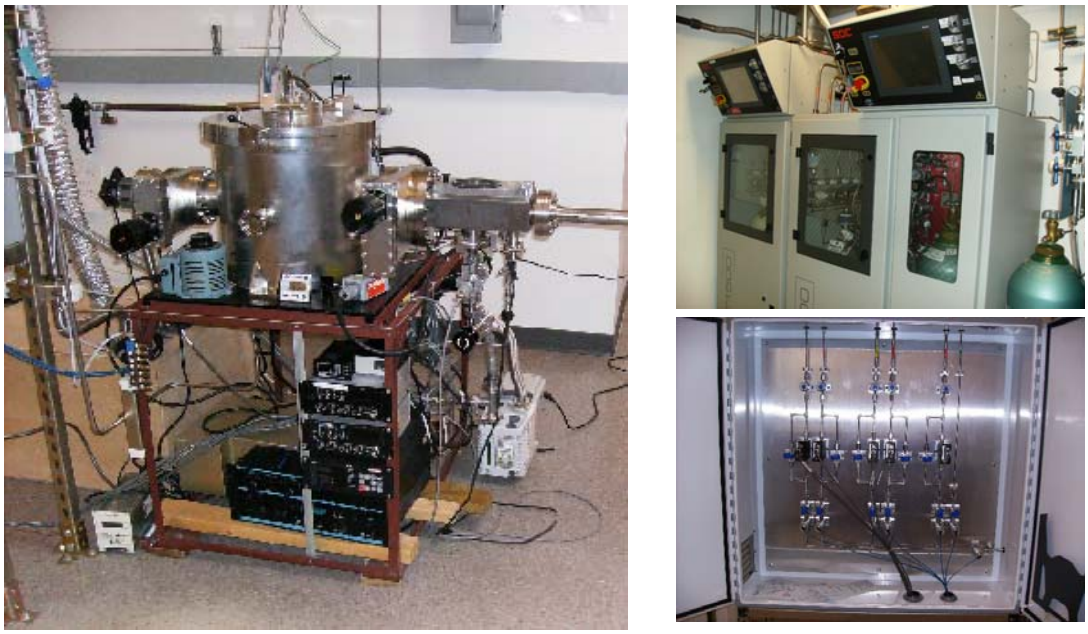

Fig. 7 Left: *a*-Si PECVD system at Solasta. Right: process gas cabinets, and process manifold, to facilitate *a*-Si PECVD deposition.

Initially, we fabricated cells using intrinsic *a*-Si, meaning in the Schottky configuration. This process was used for both nanocoax cells built off carbon nanotubes, and planar (not nanostructured) cells built in the conventional configuration. Our initial baseline for this stage was approximately 1% efficiency for Schottky nanocoax cells, versus 0.1% efficiency for Schottky planar cells (see below). In order to be in position to select the proper preparation conditions for maximum silicon PV performance, we quickly began to prepare for the introduction of dopant materials into this silicon PV medium, in order to prepare *p*-*n* and/or *p*-*i*-*n*-type junctions with our nanocoax architecture. In doing so, we continually maintained a program of establishing our baseline efficiency performance and identifying loss sources.

To summarize this PV section, we undertook the following investigations as part of this project. We show more representative results of these efforts after describing the activities associated with the final layer, the top contact.

- starting with Schottky: prepared and characterized planar and nanocoax Schottky cells
- prepared for introduction of *p* and *n* dopants to chamber:
    - purchased and configured dopant gas sources, gas cabinets and gas lines

- tested gas configurations on planar substrates
- investigated varying *p* and *n* concentrations on planar substrates
- established baseline efficiency of doped films on planar substrates
- tested dopant gas configurations on CNT-based nanocoax substrates
- investigated varying *p* and *n* concentrations on CNT-based nanocoax substrates, with and without SOG
- investigated modified doping of the *n* window layer to increase its transparency.

5. Top Contact

The final step in the fabrication of a nanocoax solar cell is the top contact. As mentioned above, we started in the classic coax configuration. Here, a large number of materials are candidate materials for the top contact. We primarily employed aluminum films. For the distributed nanocoax configuration, the requirements are that this contact be transparent as well as conducting. In other words, it should be a transparent conductive coating (TCC). Over the project period to date, we have extended considerable effort toward preparing TCCs that are conformal within our nanostructured, distributed coax architecture, with varying degrees of success.

Again, ITO was the prime candidate as the TCC of choice. As with the early effort at directly coating CNTs with ITO, we investigated various deposition methods, including thermal evaporation, electron beam evaporation, and sputter deposition. The first order of business was to optimize the deposition parameters, using information gained from characterizing the electrical conductivity and optical transparency of the ITO, using planar substrates. These two competing qualities need to be simultaneously optimized, or at least an optimal balance struck between them. To this end, we ran extensive tests of our ITO films until we reached an acceptable set of process conditions. An example of the films resulting from various process conditions is shown in Fig. 8 below.

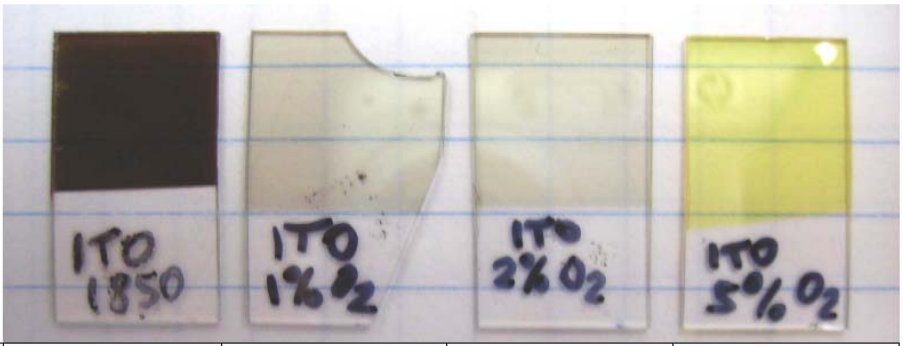

base press. [Torr]	$9x10^{-7}$	$1x10^{-5}$	$1x10^{-5}$	$1x10^{-5}$
O_2 content [%]	0.2	1.0	2.0	5.0
dep. time [min.]	240	60	60	60
thickness [nm]	1850	1000	1080	900
resistivity [Ω]	5.7	9	9	$2x10^{7}$

Fig. 8 Optical images, with sputter deposition process conditions, for four ITO films, showing the tradeoff between optical transparency and electrical conductivity.

As part of our effort on Tasks 1-1 through 1-4, as well as in preliminary work on Task 2-1 (*Optimize Performance by Varying Nanocoax Dimensions and Array Geometry)*, our appreciation for the critical nature of the properties of the TCC layer has increased. We have thus expended considerable effort attempting to improve not only the conductivity and transparency of our sputtered ITO, but also its conformality, exploring a wide parameter space. This included varying target size, substrate size, chamber pressure, sputter gun voltage, substrate-target spacing, substrate tilt angle, rotating vs. nonrotating substrate, etc. The situation has garnered so much of our attention that it has led us to investigate deposition methods other than sputtering. For example, there are known to be film deposition processes that are significantly more conformal than simple evaporation, which is directional and therefore poorly conforming to textured surfaces, and sputtering, which while somewhat omnidirectional, may not be sufficiently conformal. These include atomic layer deposition (ALD), sol-gel deposition, chemical bath deposition (CBD), and chemical vapor deposition (CVD), among others. To this end, we have we have begun to assemble a CVD system on site at Solasta that will be used to develop doped ZnO CVD as a conformal transparent conductor coating of nanopillars in array form. A photograph of this system appears below, Figure 9.

Fig. 9 CVD system being assembled at Solasta for development of conformal TCC. The initial target material will be Al-doped ZnO.

In addition, in order to accelerate the path to the best TCC solution, we have established collaborations with several research institutions in the US and Europe. The 1st is at NREL, where much of the nation's best expertise in CVD of TCO's exists; the 2nd is at another DOE lab, ANL, where promising work on conformal ITO is being developed; the 3rd is at a CRISP-funded laboratory at CSM, where CVD TCO work is ongoing, and the 4th is at the institution in Switzerland that holds the world record for amorphous silicon solar cells. The institutions and contact individuals are listed below.

Collaborating Organization Principal Investigator	Location	Activity
National Renewable Energy Laboratory (NREL) Dr. David Ginley Dr. John Perkins Dr. Thomas Gennett Dr. Tim Gessert	Golden, CO	Evaluation of DC, RF, magnetron sputtering as a route to ultraconformal transparent conductive coatings on nanopillars, using ITO, IZO and others
Argonne National Laboratory Dr. Jeffrey W. Elam	Argonne, IL	Evaluation of atomic layer deposition (ALD) as a route to ultraconformal coating on nanopillars, using ITO
Colorado School of Mines Dr. Colin Wolden	Golden, CO	Evaluation of chemical vapor deposition (CVD) as a route to ultraconformal transparent conductive coatings on nanopillars, using ZnO and others
University of Neuchatel Dr. Franz Haug Dr. Christophe Ballif	Neuchatel, Switzerland	Evaluation of chemical vapor deposition (CVD) as a route to ultraconformal transparent conductive coatings on nanopillars, using ZnO

6. Cells

Penultimately, we show below evidence for the progress made during the FutureGen grant period made, incorporating the five process steps above into completed nanocoax solar cells. As mentioned, our initial cells were Schottky junctions, with undoped *a*-Si deposited on either ITO (classic flow) or Al, Ti or Ag (distributed flow) as bottom contact, followed by Al (classic) or ITO (distributed) top contact. The Schottky cell efficiencies were clearly unimpressive (all below 1%). Moreover, there was little consistency between individual contacts on discrete cells, and between cells. Nonetheless, it was universally so that the nanocoax cells outperformed their planar counterparts, typically by a factor of 10. Thus, we were not particularly discouraged.

An example of our early Schottky results is shown in Figure 10 below. The planar cell result shown has an efficiency of under 0.1% (about 0.085%), while the nanocoax cell, with approximately the same thickness *a*-Si absorber, had an efficiency more than 20x higher, ~0.2%. This was typical for the entire series of Schottky junction cells, and was not really surprising. The main purpose was to get the *a*-Si deposition going while we prepared to optimize our arrays, our bottom and top contacts, and the layout requirements for doping.

These doping requirements were eventually met, and *p* and *n* doping gases were obtained and plumbed into our PECVD system. We installed process lines for diborane and phosphene, with hydrogen and nitrogen for dilution as needed. The first set of doped structures yielded immediate improvements in all PV parameters, though with obvious need of optimization. The initial results on planar and nanocoax cells can be seen in Figure 11. These data continue to show a performance advantage (1.4/0.33 ~ 4x) of the nanocoax over the planar configuration.

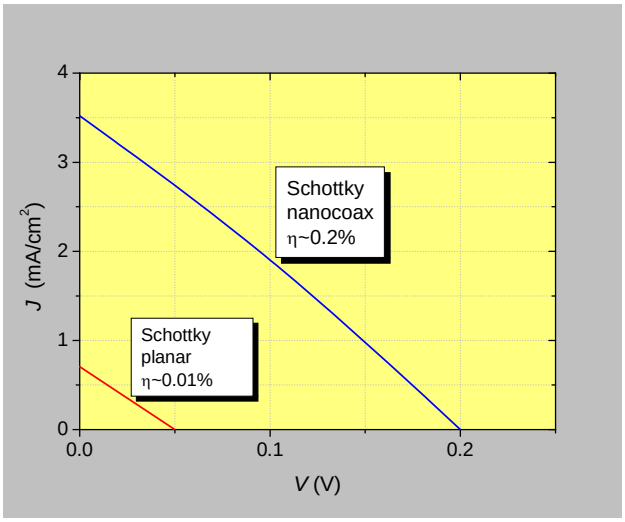

Fig. 10 Representative initial results for Schottky solar cells, in planar and Solasta configurations, using ITO and Al as contact metals, and comparable thickness *a*-Si for both.

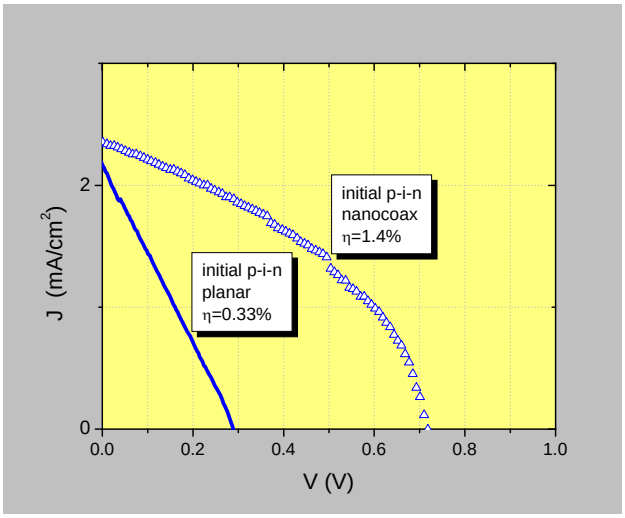

Fig. 11 Representative initial results for *p-i-n* solar cells, in planar and Solasta configurations, with comparable thickness *a*-Si for both. The efficiencies shown are typical for such early-stage, unoptimized cells.

Since doping was first incorporated into our *a*-Si deposition process, we have run through several hundred iterations of process parameters and conditions, including those associated with the bottom and top contacts. To reiterate comments offered in a previous quarterly report, we encountered along the way various problems that have impacted progress, such as current leakage, possibly due to defects in the CNT arrays, and inadequate electrical conductivity, transmittance and especially conformality of our ITO TCC. Certain actions were taken to remediate these problems, such as the introduction of the SOG step, which we continue to evaluate. Our cell efficiencies have gradually increased, from the 2% to the 5% range, though consistency and reproducibility are important issues that need to be addressed. As an example of one of our better cells, we show in Figure 12 data for one sample with four contacts, each of area 0.085 cm^2, that performed similarly under AM1.5 simulated light. This cell had an average efficiency of η=5.27%, with good consistency in J_{sc} and V_{oc}. Also shown for comparison in the figure is the state-of-the-art for single junction *a*-Si solar cells, by the Neuchatel group, with η~9.5%. To date, our cell with a "champion" contact, which unfortunately is indeed the only one of its kind (other contacts on same cell performing not nearly as well), possesses an efficiency of 6.47%. On the other hand, individual contacts on other cells have independently demonstrated higher J_{sc}'s (up to 15 mA/cm^2) and V_{oc}'s (up to 0.8V), both close to the record values. We anticipate that once all the various sources of efficiency loss in the nanocoax solar cell are identified and eliminated, we will significantly exceed the above world record.

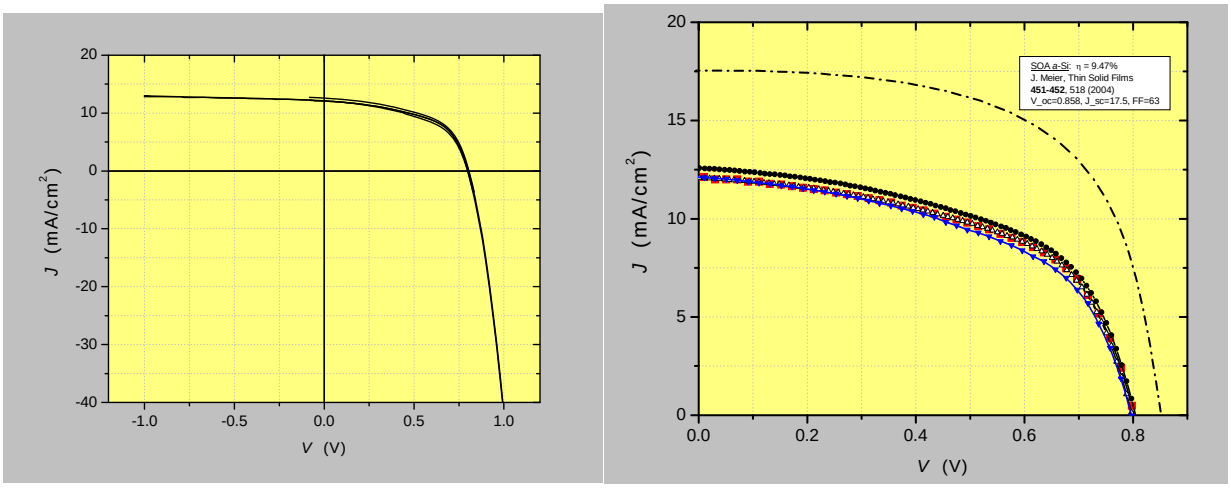

Fig. 12 Current density – voltage traces for four contacts on a nanocoax solar cell under AM1.5 illumination, on (left) expanded and (right) PV-relevant scales. Consistent PV performance is observed, with η_{avg}=5.27±0.21%. Also shown for comparison is a facsimile curve of the Neuchatel world record for single-junction *a*-Si solar cells, η=9.5%.

We have also been able to make a comparison between the performance of a nanostructured solar cell and a conventionally-prepared, planar solar cell having comparable thickness *a*-Si. In Figure 13, it can be seen that the Solasta cell significantly outperformed the planar cell: by more than 100% in current (J_{sc}). This can be explained as follows: in the planar cell, the *i*–layer in the *a*-Si PV medium is too thin to efficiently absorb enough light to be able to generate a large number of charge carriers. Thus, its efficiency is below what would normally be achievable with a proper thickness cell. The Solasta cell, on the other hand, is able to collect more light in spite of having the same thickness PV absorber as the planar cell, due to its nanostructured architecture. This means that the Solasta cell is more than a different geometry, which can explain only part of the light collection difference. It is also an array of subwavelength waveguides, which are able to efficiently couple to and absorb visible radiation to an extend defined not only by the absorber thickness, but also by the array architecture (symmetry and pitch). Optimization of these latter aspects is the domain of later tasks.

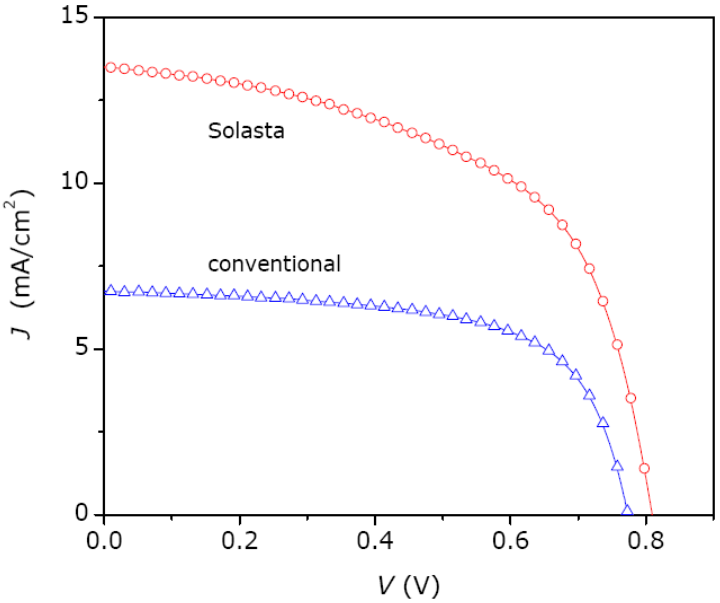

Fig. 13 Comparison of photovoltaic characteristics of Solasta and planar (conventional) solar cells having the same *a*-Si absorber thicknesses. The former markedly outperforms the latter.

7. Simulations

In this Task effort, we have initiated a program to develop an understanding of electromagnetic wave propagation in individual nanoscale “co-metal” structures, such as nano-striplines and nanocoaxes. Ultimately, both the polaritonic and plasmonic regimes of operation need to be investigated, and the range of the transverse electromagnetic (TEM)-like polaritonic mode propagation determined. This needs to be done not only in individual structures, but in assemblies (arrays) of such. Simultaneously, we are in the process of developing FDTD (finite difference time domain) codes based on the MEEP (MIT electromagnetic equation propagation) software platform. These will eventually be tested against calculations on single nano co-metal structures. To date, our preliminary developed codes have been applied to nanocoax structures in cell configurations approximating those anticipated for the solar cells, using monochromatic(single wavelength) light. We have been able to obtain electromagnetic field distributions with this simulation process, an example of which is shown in Fig. 14. Here, the electromagnetic wave (with electric field magnitude and direction color encoded), propagates at an angle from above, through a non-optimized, conventional nanocoax array. Clearly visible is the transformation of the wave as it enters the nanocoaxes, as well significant back reflection, illustrated by a standing wave pattern.

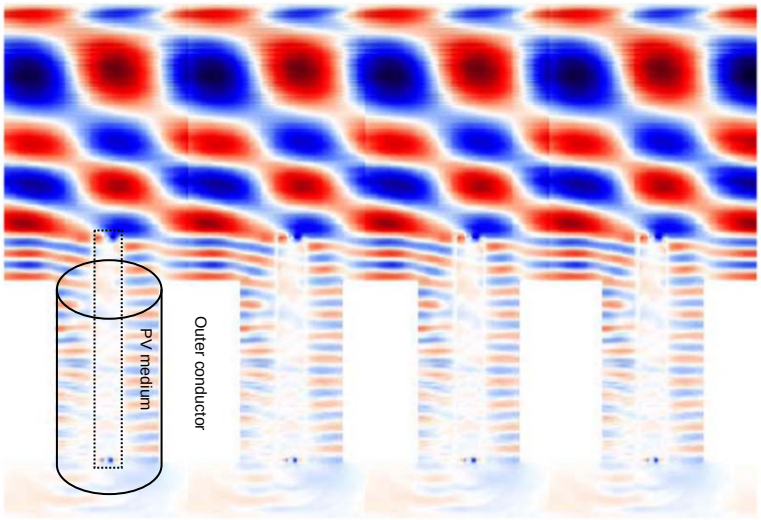

Fig. 14 Computer generated simulation of 500 nm light propagation (from above) into an array of nanocoaxial structures, plotting the electric field amplitude *E* (red and blue indicating + and – sign of *E*). The outline of one coax is shown on the left, where the components of the structure are indicated.

This plot shows the power of the FDTD codes being developed, and the type of calculation and simulation that can be further developed, moving forward, to obtain a powerful, multiwavelength set of codes for arbitrary nanocoax configuration. This will allow, ultimately, a type of reverse engineering to be incorporated into our development scheme, toward a computer design of Solasta cells with optimized response.

Products: Other than the collaboration list above, no products (publications, inventions, databases, websites, etc). were developed under this award.